Available online at www.sciencedirect.com
ScienceDirect
Trans. Nonferrous Met. Soc. China 34(2024) 1016−1026
Transactions of Nonferrous Metals Society of China
www.tnmsc.cn

Dissolution behavior and improvement approach for gallium extraction from zinc refinery residues

Wei ZHANG[1,2], Shuai RAO[3], Li-qing LI[1], Xiao-dan GONG[2], Cai-gui WU[2], Dong-feng HU[2], Hong-yang CAO[3], Zhi-qiang LIU[3]

1. Faculty of Materials Metallurgy and Chemistry, Jiangxi University of Science and Technology, Ganzhou 341000, China;
2. Danxia Smelter, Shenzhen Zhongjin Lingnan Nonfemet Co., Ltd., Shaoguan 512325, China;
3. Institute of Resource Utilization and Rare Earth Development, Guangdong Academy of Sciences, Guangzhou 510650, China

Received 7 September 2022; accepted 21 March 2023

Abstract: Aiming at solving low Ga leaching efficiency during actual industrial production in Danxia Smelter, chemical composition, phases and morphologies of various zinc refinery residues were characterized using ICP−AES, XRD and SEM−EDS. Compared with the normal material, Ga was embedded in the jarosite phase from the special zinc refinery residue, causing difficulty in Ga leaching. During the oxidation pressure leaching, the dissolution behaviors of Ga, As and Fe presented similar variation tendency. Namely, a sufficient H_2SO_4 concentration and liquid-to-solid ratio promoted the dissolution of Ga, Fe and As, whereas higher reaction temperature and oxygen partial pressure weakened the leaching. Based on the results, leaching parameters were optimized for enhancing Ga recovery. Through weakening the 1st oxidation pressure leaching (by decreasing reaction temperature and total pressure to 90 °C and 0.2 MPa, respectively) and strengthening the 3rd atmospheric leaching (by increasing H_2SO_4 concentration and reaction temperature to 160 g/L and 85 °C, respectively), the leaching efficiency of Ga increased from 77.83% to 96.46%.
Key words: dissolution behavior; zinc refinery residue; gallium; jarosite; scorodite

1 Introduction

Gallium (Ga) is widely used in high-tech products such as integrated circuits and advanced electronic devices [1,2]. The end-use of GaAs and GaN in integrated circuits accounts for about 74% of the total U.S. gallium consumption owing to high computation speed [3]. As a typical scattered metal, Ga is commonly associated with bauxite [4], sphalerite [5], iron ore [6] and coal [7], etc. Therefore, Ga is primarily recovered as a by-product from the metallurgy of aluminum [8,9], zinc [10,11], and the processing of coal [12,13].

The comprehensive recovery of Ga from non-ferrous minerals follows the strategy of gradual enrichment. Meanwhile, Ga enrichment carrier strongly depends on the technological route for extracting main metals such as Zn. During zinc pyrometallurgy, more than 95% of Ga is enriched in the water-quenched slag with an average content of 0.03−0.04 wt.%. Since Ga mainly occurs in the amorphous silicate phase, the extraction of Ga from the slag is very difficult [14]. When Zn is produced through the dominant roasting−leaching−purification−electrowinning process [15], the Ga behavior is consistent with that of Fe owing to the nearly identical size of the Ga^{3+} (0.62 Å) and Fe^{3+}

Corresponding author: Shuai RAO, Tel: +86-15084917790, E-mail: 491660987@qq.com;
Li-qing LI, E-mail: liliqing79@126.com
DOI: 10.1016/S1003-6326(23)66450-7

(0.64 Å) [16]. Above 98% of Ga remains in the leaching residue, which is closely associated with $ZnFe_2O_4$ phase [17,18]. And then, reduction volatilization or hot acid leaching is employed to treat the residue. Only 10%−15% of Ga volatilizes into the crude zinc oxide dust, causing a huge Ga loss [14]. Above 90% of Ga and Fe are dissolved into the solution through hot acid leaching. However, the separation of Zn and Fe is conducted by precipitation as jarosite [16], resulting in the co-precipitation of Ga and Fe. To date, comprehensive recovery of Ga still cannot be commercially employed in the course of the dominant zinc extraction route.

Compared with atmospheric leaching, pressure leaching is considered more suitable for treating the Ga-rich zinc concentrate owing to the absence of roasting procedure [14]. More than 90% of Ga and Fe are directly leached into the solution. Before removing Fe, Ga is successfully enriched in refinery residues with an average grade ranging from 0.2 to 0.5 wt.% through pre-neutralization and zinc powder replacement [19]. In order to further recover Ga from zinc refinery residues, some researches were conducted including pressure leaching [20], stepwise leaching [21,22] and complex-leaching [23]. These methods indicate a higher Ga leaching efficiency on a laboratory scale. For instance, more than 98% of Ga was leached in a 156 g/L H_2SO_4 solution at 150 °C for 3 h with a liquid-to-solid ratio of 8 mL/g [20].

In southern China, zinc sulfide concentrates with a higher Ga content (above 100 g/t) are produced from Fan Kou Lead and Zinc Mine. Based on the resource characteristics, a novel technological route, which incorporates leaching of zinc refinery residues, solvent extraction and electrowinning, is established in Danxia Smelter and enables an annual production of 15 t Ga [24]. However, Ga leaching efficiency varies from 70% to 90%, causing an unstable production. It is necessary to figure out the reasons and improve Ga leaching efficiency. In this study, various zinc refinery residues (obtaining lower or higher Ga recovery) were characterized using ICP−AES, XRD and SEM−EDS. During the oxidation pressure leaching, the main influential factors including H_2SO_4 concentration, oxygen partial pressure, reaction temperature and liquid-to-solid ratio on the dissolution behaviors of Ga, Fe, and As were investigated in detail.

2 Experimental

2.1 Materials

Zinc refinery residues were provided from Danxia Smelter, China. Leaching solution was prepared with analytical-grade H_2SO_4 and deionized water. The purity of oxygen used was above 99%.

2.2 Experimental procedure

Oxidation pressure leaching experiments were conducted through modelling industrial conditions to understand the limit of Ga leaching. To study main influential factors on the dissolution behaviors of Ga, As and Fe, a series of leaching experiments were conducted in a 250 mL Hastelloy autoclave with reaction time of 2 h.

2.3 Characterization and analysis

Chemical compositions of the leaching solution and leaching residue were analyzed using ICP-AES (Spectro Acros). The phase, morphology and micro-structural analyses of the sample were carried out through XRD (Bruker D8 Advance) and SEM−EDS (FEI Quanta 650; Bruker Quantax), respectively.

3 Results and discussion

3.1 Actual technological route for leaching of zinc refinery residues

Zinc refinery residues are typical by-products derived from the purification of zinc leachate through adding zinc powder. They usually contain valuable elements such as Zn, Cu, Ga and Ge, which mainly occur in the form of metals, oxides, sulfides and silicates [25]. Owing to different leaching behaviors of Ga and Ge in a H_2SO_4 solution, multi-stage counter current leaching (Fig. 1) is proposed to treat zinc refinery residues for the comprehensive recovery of Cu, Ga and Ge [26,27]. Table 1 lists main parameters for the counter current leaching process. Zinc refinery residues were leached in the first autoclave to yield a suitable solution for the subsequent solvent extraction, requiring relatively low concentrations of final H_2SO_4 (20−30 g/L) and Fe^{2+} (<1 g/L). Compared with the 1st leaching, the 2nd leaching

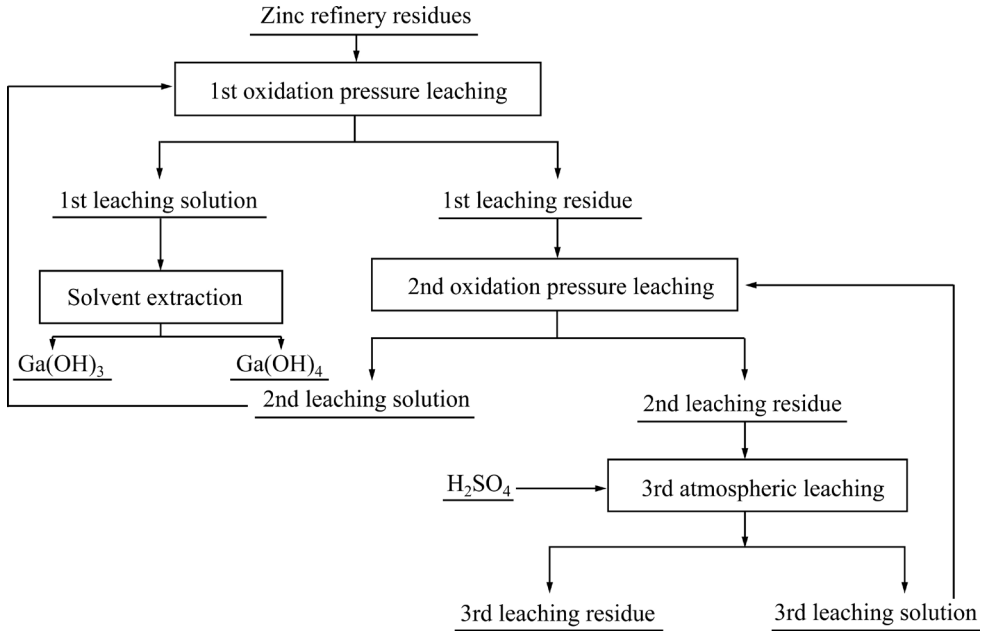

Fig. 1 Technological route for leaching of zinc refinery residues

Table 1 Main parameters for leaching of zinc refinery residues

Procedure	Reaction temperature/°C	Reaction pressure/MPa	Oxidization agent	Reaction time/h	Initial H_2SO_4 concentration/(g·L^{-1})	Final H_2SO_4 concentration/(g·L^{-1})
1st	105−115	0.2−0.3	O_2	4−6	110−130	20−30
2nd	115−125	0.25−0.35	O_2	4−6	140−160	110−130
3rd	25	−	−	1−2	150−170	140−160

presented higher reaction temperature (115−125 °C) and reaction pressure (0.25−0.35 MPa) to promote the dissolution of insoluble metals and sulfides. In the 3rd leaching tank, fresh H_2SO_4 solution was used as the leaching agent to dissolve Ga and Ge adequately.

3.2 Various Ga leaching results for actual production

3.2.1 Leaching of normal zinc refinery residue with high Ga extraction

Based on the technological route from Fig. 1, normal production results for leaching of zinc refinery residues are listed in Table 2. As usual, the content of Ga in the 3rd residue was lower than 0.1 wt.%. Moreover, Cu, Zn and Fe were also leached adequately.

XRD patterns of the normal zinc refinery residue and 3rd leaching residue are shown in Fig. 2. It can be seen from Fig. 2(a) that the zinc refinery residue was composed of SiO_2, $PbSO_4$ and $Zn_3Cu_2(SO_4)_2(OH)_6{\cdot}4H_2O$. No characteristic peaks of Ga and Ge compounds were detected owing to their low contents. After leaching, the characteristic peaks of Cu and Zn compounds disappeared. The main phases in the 3rd leaching residue were $PbSO_4$ and SiO_2, as shown in Fig. 2(b).

Table 2 Leaching results of normal zinc refinery residue

Element	Content in material/wt.%	Content in 3rd leaching residue/wt.%	Leaching efficiency/ %
Cu	10.81	0.59	97.54
Zn	14.06	0.74	97.63
Fe	2.23	0.45	90.91
Ga	0.76	0.08	95.26
Ge	0.51	0.29	74.39
Pb	2.99	6.65	0
As	1.24	0.4	85.47

Figure 3 indicates SEM images of the normal zinc refinery residue and the 3rd leaching residue.

The zinc refinery residue contained many gray blocky-shaped particles (Spots 1, 3 and 4) and bright tiny particles (Spot 2). Based on EDS results from Table 3, these gray particles presented similar composition including O, S, Cu, Zn, confirming the formation of sulfates. No Ga- or Ge-rich particles were observed in Fig. 3(a). Ga and Ge were discretely distributed in these blocky-shaped particles. Spot 2 belonged to $PbSO_4$ phase owing to the presence of Pb, S and O. After completing leaching, the dominant phase in the 3rd leaching residue was dark silica gel with tiny particle size (Spots 7 and 8). A higher content of Ge was detected in these particles due to the formation of germanium−silica gel [28]. Insoluble gahnite particles such as Spot 5 and Pb-rich particles such as Spot 6 were also observed in Fig. 3(b).

3.2.2 Leaching of special zinc refinery residue with low Ga extraction

As shown in Table 4, a relatively high content

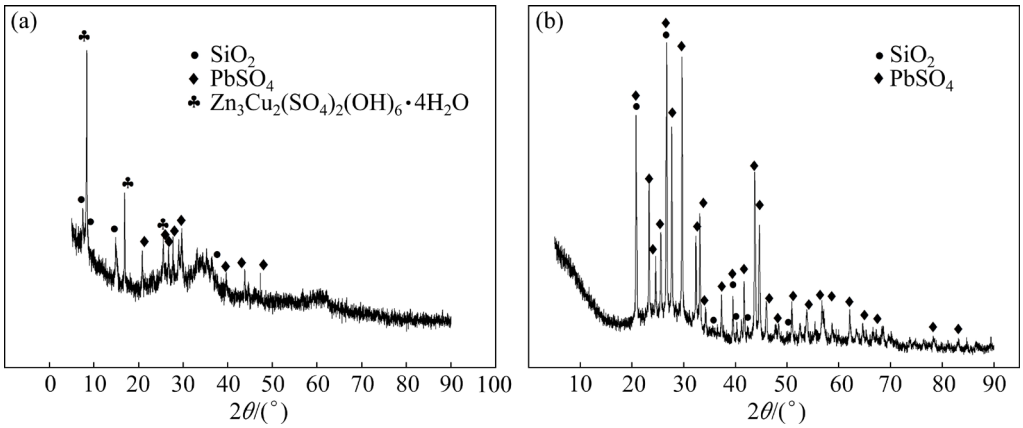

Fig. 2 XRD patterns of normal zinc refinery residue (a) and the 3rd leaching residue (b)

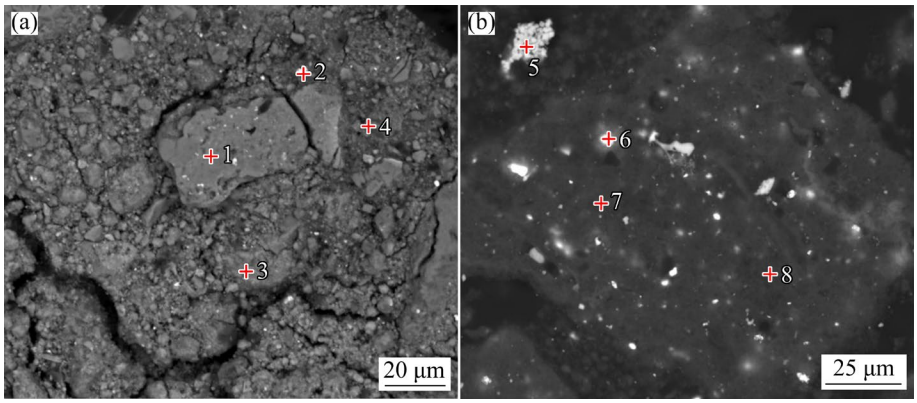

Fig. 3 SEM images of normal zinc refinery residue (a) and the 3rd leaching residue (b)

Table 3 Chemical compositions of selected particles from Fig. 3 (wt.%)

Spot No.	O	Al	Si	S	Fe	Cu	Zn	Ga	Ge	As	Sb	Pb
1	28.89	2.53	2.62	4.72	0.88	10.38	34.64	1.15	1.99	4.32	−	−
2	21.79	−	−	9.29	1.03	4.42	5.93	−	−	−	−	51.46
3	33.32	1.36	7.81	6.22	1.52	18.02	17.95	0.95	0.48	3.53	−	−
4	33.24	2.81	3.59	8.18	1.89	12.69	24.11	0.71	0.72	4.44	−	−
5	34.09	15.4	7.05	1.19	−	4.72	36.03	−	−	0.5	0.37	−
6	33.67	−	18.65	5.03	−	0.41	0.2	−	0.54	2.25	2.15	23.52
7	47.73	0.83	32.22	4.26	0.31	0.68	2.5	−	1.3	1.84	3.49	0.96
8	48.2	0.39	33.26	4.06	0.32	0.75	0.73	−	0.93	2.04	3.67	1.38

Table 4 Leaching results of special zinc refinery residue

Element	Content in material/wt.%	Content in 3rd leaching residue/wt.%	Leaching efficiency/%
Cu	10.51	0.92	95.98
Zn	15.32	1.25	96.26
Fe	2.98	1.51	76.76
Ga	0.6	0.29	77.83
Ge	0.46	0.38	62.11
Pb	2.84	6.2	0
As	2.8	1.82	70.18

of As (above 2.8 wt.%) was detected in the special zinc refinery residue compared with the normal material. After leaching, about 0.3 wt.% of Ga remained in the 3rd leaching residue. Moreover, the leaching efficiency of As and Fe was also lowered to 76.76% and 70.18%, respectively.

Compared with Fig. 2, XRD patterns (Fig. 4) presented new characteristic peaks of jarosite ($KFe_3(SO_4)_2(OH)_6$) and iron sulfate hydroxide ($Fe_4(OH)_{10}SO_4$) in the special material and the 3rd residue.

Figure 5 shows SEM images of the special zinc refinery residue and the 3rd leaching residue. Based on EDS results from Table 5, Spot 1 contained an especially high content of Ga. Moreover, paragenetic relationship was also found among Ga, Al, Fe, S and O, as shown in Fig. 6. It can be confirmed that Ga was mainly embedded in the jarosite phase. The result was consistent with previous research which reported that Ga^{3+} replaced Fe^{3+} in the jarosite structure to form a nearly ideal solid solution series, as expressed in Reactions (1) and (2) [16]. The main phases at Spots 2 and 3 were elemental copper and copper sulfide, respectively. Spot 4 was viewed as zinc aluminate gahnite owing to high contents of Al, Zn and O. Spot 5 represented a Ge-rich particle containing high contents of Cu, Fe and Zn. Spots 6 and 7 were silica gel particles, causing a strong adsorption of Ge. After completing leaching, except for similar particles including $PbSO_4$ (Spot 9), $ZnAl_2O_4$ (Spot 10) and germanium–silica gel (Spot 11), containing Ga and As particles such as Spots 7 and 8 were also observed in Fig. 5(b).

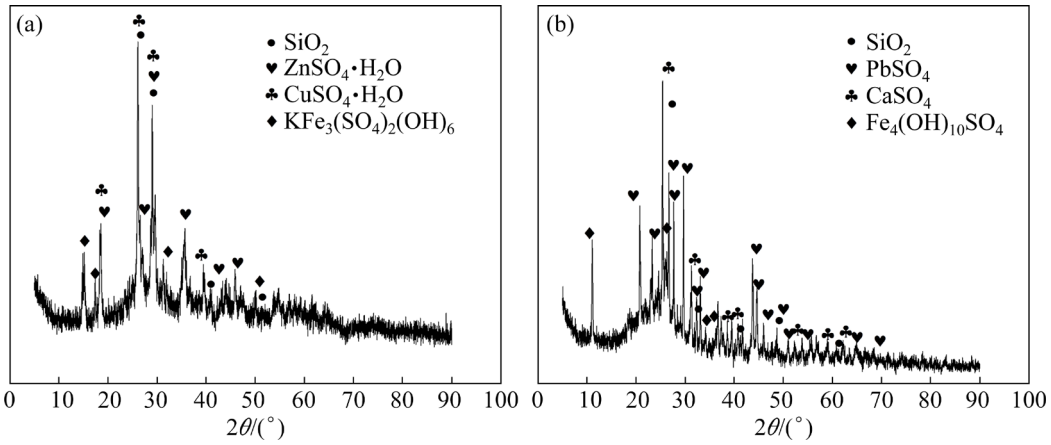

Fig. 4 XRD patterns of special zinc refinery residue (a) and the 3rd leaching residue (b)

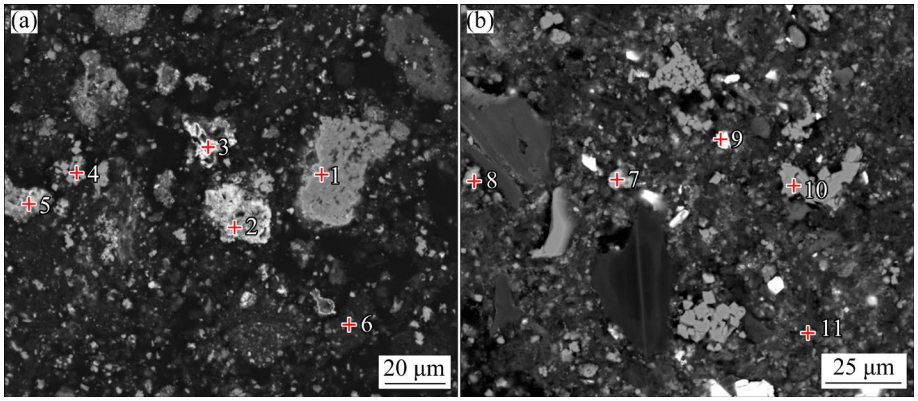

Fig. 5 SEM images of special zinc refinery residue (a) and the 3rd leaching residue (b)

Table 5 Chemical compositions of selected particles from Fig. 5 (wt.%)

Spot No.	O	Al	Si	S	K	Fe	Cu	Zn	Ga	Ge	As	Pb
1	40.84	9.11	5.97	10.71	3.75	2.6	1.98	6.87	10.07	−	−	5.42
2	−	−	−	11.92	−	1.44	86.64	−	−	−	−	−
3	7.1	0.97	1.23	0.39	−	1.07	88.42	−	−	−	−	−
4	33.16	25.39	0.31	−	−	3.6	0.84	36.69	−	−	−	−
5	29.52	1.56	4.05	2.28	−	16.69	12.12	9.96	−	5.69	11.29	−
6	43.55	2.67	27.97	1.16	0.31	2.72	7.07	4.87	0.56	1.02	4.21	−
7	31.35	2.73	3.98	3.01	0.82	3.92	0.37	2.44	1.19	0.39	14.03	8.72
8	29.94	−	2.01	1.29	0.27	5.51	−	1.64	0.37	0.15	24.97	5.54
9	19	−	0.68	8.36	0.22	0.32	−	−	−	−	−	70.18
10	33.13	25.74	−	−	−	3.03	−	37.87	−	−	−	−
11	43.39	0.91	27.37	2.01	−	1.66	−	1.42	−	1.37	6.73	4.55

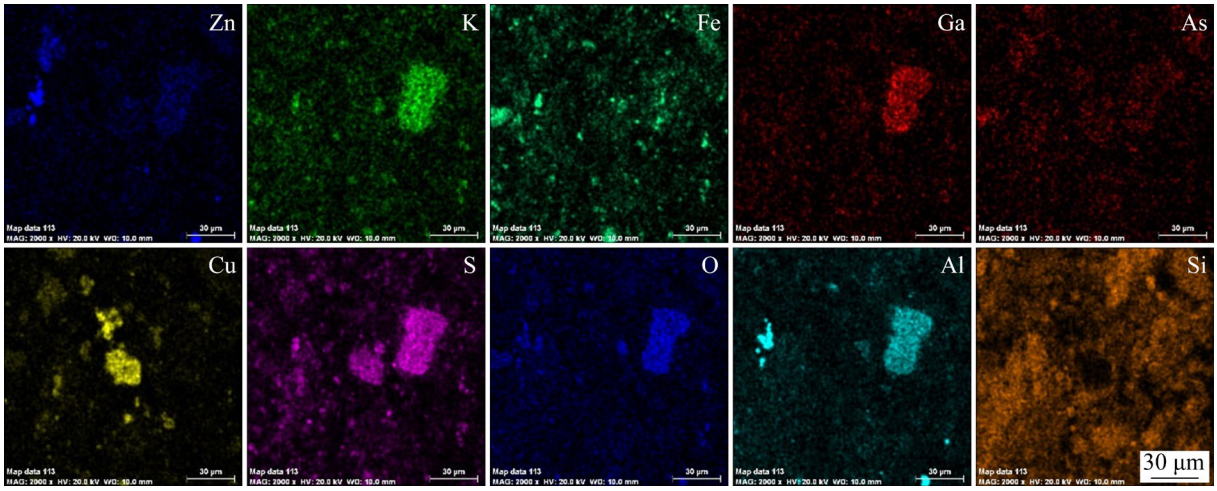

Fig. 6 Main elemental surface distribution in special zinc refinery residue

$$K_2SO_4+3Fe_2(SO_4)_3+12H_2O \rightleftharpoons 2KFe_3(SO_4)_2(OH)_6+6H_2SO_4 \quad (1)$$

$$K_2SO_4+3Ga_2(SO_4)_3+12H_2O \rightleftharpoons 2KGa_3(SO_4)_2(OH)_6+6H_2SO_4 \quad (2)$$

3.3 Leaching efficiency of Ga

3.3.1 φ−pH diagram of Ga−As−Fe−H_2O system

Figure 7 illustrates φ−pH (φ is the potential) diagram for As−Fe−Ga−H_2O system with $[As]_T$= 1 mol/L, $[Fe]_T$=1 mol/L and $[Ga]_T$=0.01 mol/L at 120 °C. Atmospheric leaching of zinc refinery residues could bring about higher Ga and Fe leaching efficiencies owing to the presence of Fe^{2+}, as reported from previous researches [21,22]. During actual production, oxidation pressure leaching was conducted to treat zinc refinery residues for highly effective recovery of Cu. Moreover, it was expected that Fe^{3+} should be predominant in the 1st leaching solution with Fe^{2+} concentration below 1 g/L, which was beneficial to Fe removal during the subsequent solvent extraction. When the special refinery residue contained a higher content of As, the transformation from As^{3+} to As^{5+} and Fe^{2+} to Fe^{3+} easily occurred during the oxidation pressure leaching [29]. Simultaneously, $FeAsO_4$ and $GaAsO_4$ precipitates were produced in pH range from 0 to 2.0. The main chemical reactions for the formation of $FeAsO_4$ and $GaAsO_4$ were expressed as Reactions (3) and (4). Based on the thermodynamic analyses, the effective measures for preventing precipitation reactions were to improve H_2SO_4 concentration and reduce oxygen partial pressure.

$$4Fe^{2+}+4HAsO_2+3O_2+10H_2O \rightleftharpoons 4FeAsO_4\cdot 2H_2O+8H^+ \quad (3)$$

$$4Ga^{3+}+4HAsO_2+2O_2+12H_2O \rightleftharpoons 4GaAsO_4\cdot 2H_2O+12H^+ \quad (4)$$

3.3.2 Dissolution behavior of Ga, As and Fe

A series of leaching experiments were conducted on a laboratory scale, and the results are shown in Fig. 8. The concentrations of Ga, As and Fe in the leachate showed a similar variation tendency when leaching conditions including H_2SO_4 concentration, oxygen partial pressure, temperature and liquid-to-solid ratio changed. Namely, an increasing H_2SO_4 concentration and liquid-to-solid ratio enhanced the dissolution of Ga, As and Fe. A sufficient H_2SO_4 concentration could ensure soluble Ga^{3+}, As^{5+} and Fe^{3+} in the leachate and prevent co-precipitation reactions among them.

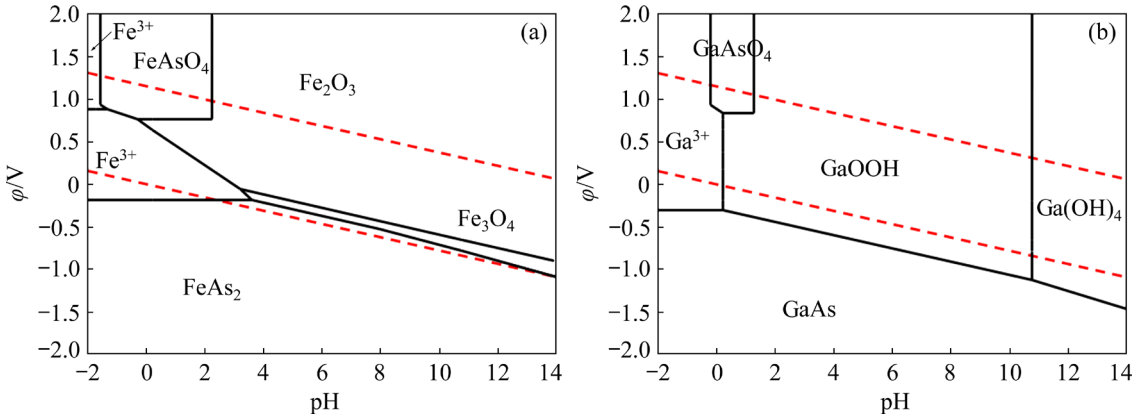

Fig. 7 φ–pH diagrams for Ga–As–Fe–H_2O system at 120 °C with $[As]_T$=1 mol/L, $[Fe]_T$=1 mol/L and $[Ga]_T$= 0.01 mol/L: (a) Fe; (b) Ga

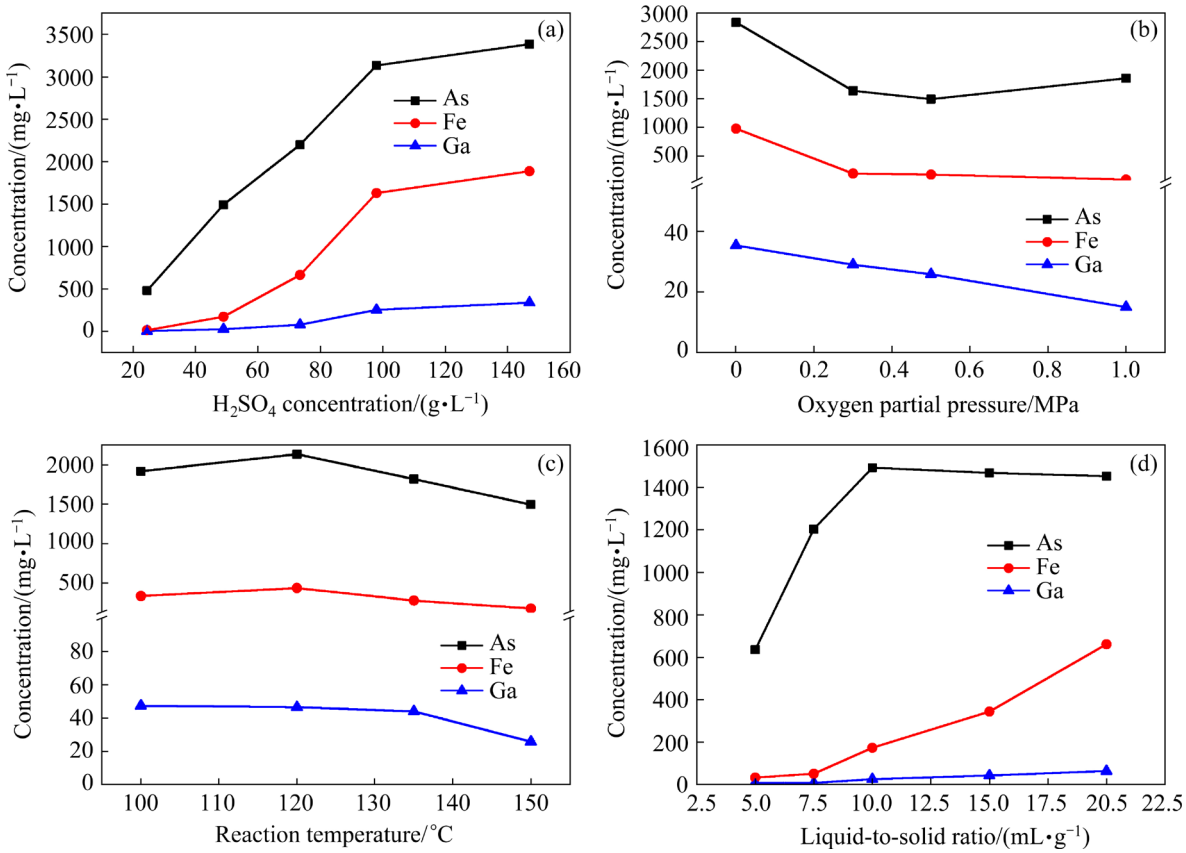

Fig. 8 Dissolution behavior of Ga, As and Fe during oxidation pressure leaching of special zinc refinery residue: (a) H_2SO_4 concentration (Operation conditions: 10 mL/g, 150 °C, 0.5 MPa); (b) Oxygen partial pressure (Operation conditions: 49 g/L H_2SO_4, 10 mL/g, 150 °C); (c) Reaction temperature (Operation conditions: 49 g/L H_2SO_4, 10 mL/g, 0.5 MPa); (d) Liquid-to-solid ratio (Operation conditions: 49 g/L H_2SO_4, 150 °C, 0.5 MPa)

However, higher oxygen partial pressure and temperature caused a reduction in concentrations of Ga, As and Fe. It was confirmed that higher oxygen partial pressure could promote the oxidation of Fe^{2+} to Fe^{3+} and As^{3+} to As^{5+}. Moreover, higher reaction temperature was beneficial to the precipitation reactions of As^{5+}, Fe^{3+} and Ga^{3+} owing to the endothermic process.

3.3.3 Co-precipitation of Ga, As and Fe

In order to further clarify co-precipitation behaviors of Ga, As and Fe, an individual pressure leaching experiment was carried out. The actual 2nd leaching solution was pre-neutralized to a final acid concentration of 30 g/L through adding the special zinc refinery residue. Then, the resulting solution after liquid−solid separation was treated with a reaction temperature of 120 °C and oxygen partial pressure of 0.3 MPa. A brown precipitate was observed in the solution, and XRD analysis (Fig. 9) confirmed the formation of scorodite. The obtained scorodite particle presented a uniform morphology, as shown in Fig. 10. EDS result from Table 6 demonstrated that the precipitate was mainly composed of O, As, Ga and Fe. The average Ga content in the precipitate was 4.69 wt.%. It can be seen from Fig. 11 that the distribution of Ga and Fe was absolutely accordant. No discrete Ga compounds were detected, indicating that Ga^{3+} substituted for Fe^{3+} in the scorodite structure.

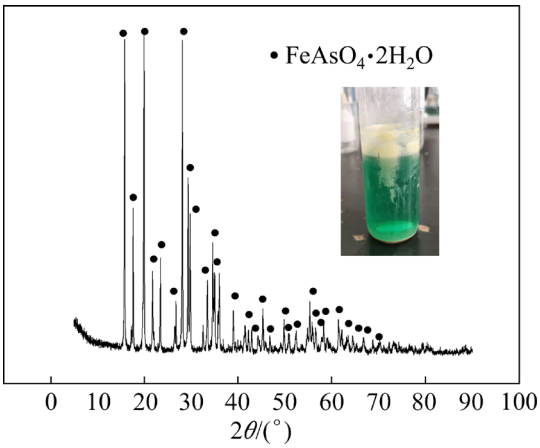

Fig. 9 XRD pattern of scorodite precipitate

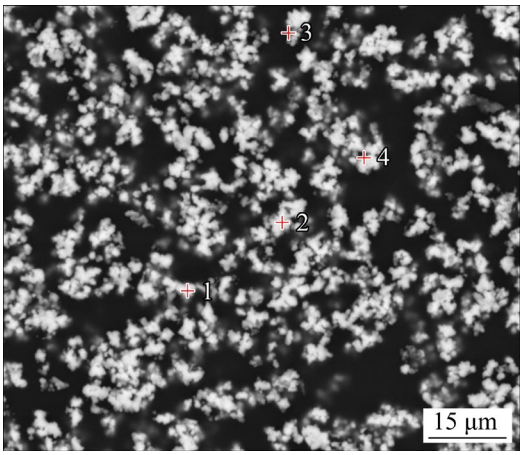

Fig. 10 SEM image of scorodite precipitate

Table 6 Chemical compositions of selected particles from Fig. 10 (wt.%)

Spot No.	O	Fe	Cu	Zn	Ga	As	Cd	Sb
1	28.92	24.27	0.74	0.73	4.49	36.51	0.39	0.94
2	28.69	23.85	0.92	0.93	4.87	36.54	0.4	1.02
3	27.61	25.08	0.86	0.75	4.93	35.33	0.47	2.13
4	25.41	26.46	0.73	0.73	4.46	36.61	0.45	1.04
Average	27.66	24.92	0.81	0.79	4.69	36.25	0.43	1.28

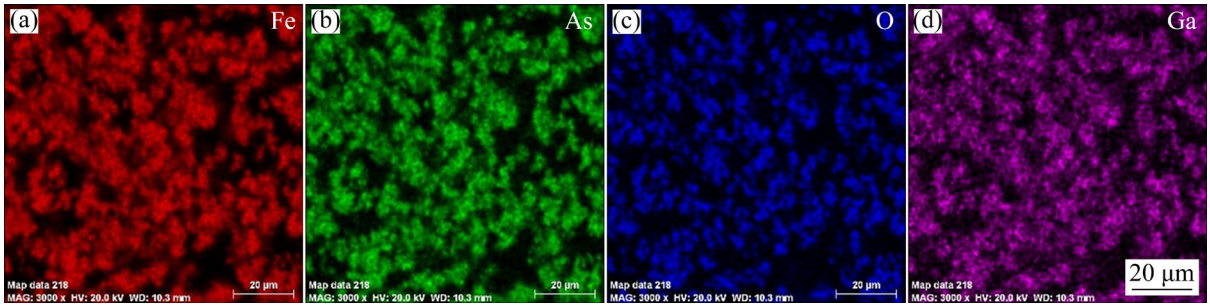

Fig. 11 Main elemental surface distribution in scorodite precipitate

3.4 Improvement approaches for Ga leaching

3.4.1 Optimization leaching parameters

Based on above-mentioned results, the low Ga leaching efficiency was attributed to the following aspects: (1) the chemical composition of the special zinc refinery residue was more complex, and Ga was embedded in the jarosite phase. In this regard, a higher H_2SO_4 concentration was required to dissolve jarosite; (2) During the oxidation pressure leaching, weak acid and strong oxidation atmosphere easily caused co-precipitation of Ga, As and Fe, resulting in a decreasing Ga leaching efficiency. Therefore, the improved methods for Ga leaching were proposed through intensifying the 3rd atmospheric leaching and weakening the 1st oxidation pressure leaching. The main parameters were optimized as follows: (1) During the 1st pressure leaching, compressed air rather than O_2 was used as the oxidizing agent with a total reaction pressure adjusted to 0.1−0.2 MPa. The reaction temperature was also decreased to 90−100 °C. (2) In order to promote the dissolution of jarosite, the 3rd atmospheric leaching was intensified by increasing H_2SO_4 concentration to 160 g/L and reaction temperature to 85 °C.

3.4.2 Actual production results

After adjusting leaching parameters, actual production results are listed in Tables 7 and 8, respectively. The concentrations of Fe, As and Ga in the leachate were improved gradually during the counter current leaching. Ga concentration remained at about 2.0 g/L in the 1st leaching solution, which was subsequently recovered through solvent extraction and electrowinning. The Ga content in the 3rd residue was below 0.05 wt.%, obtaining above 96% of Ga leaching efficiency.

Table 7 Main elemental concentrations and contents in leaching solutions by optimization parameters

Production No.	Parameter	Cu	Zn	Fe	Ga	Ge	As
Production-1#	Concentration at 1st/(g·L^{-1})	25.05	30.03	5.42	2.07	0.66	4.34
	Concentration at 2nd/(g·L^{-1})	11.57	10.44	3.44	1.12	0.54	3.51
	Concentration at 3rd/(g·L^{-1})	2.24	1.77	0.93	0.23	0.13	1.46
	Content at 1st/wt.%	53.81	65.23	36.53	45.89	18.18	19.12
	Content at 2nd/wt.%	37.25	28.87	46.31	43.00	62.12	47.24
	Content at 3rd/wt.%	8.94	5.89	17.16	11.11	19.70	33.64
Production-2#	Concentration at 1st/(g·L^{-1})	28.21	23.16	6.22	2.03	0.68	5.06
	Concentration at 2nd/(g·L^{-1})	10.81	8.21	3.43	1.03	0.45	3.63
	Concentration at 3rd/(g·L^{-1})	3.75	3.33	1.82	0.40	0.22	2.36
	Content at 1st/wt.%	61.68	64.55	44.86	49.26	33.82	28.26
	Content at 2nd/wt.%	25.03	21.07	25.88	31.03	33.82	25.10
	Content at 3rd/wt.%	13.29	14.38	29.26	19.70	32.35	46.64

Table 8 Production result for leaching of zinc refinery residues by optimization parameters

Production No.	Parameter	Cu	Zn	Fe	Ga	Ge	Pb	As
Production-1#	Content in raw material/wt.%	10.5	12.02	3.06	0.64	0.52	2.11	2.09
	Content in 3rd leaching residue/wt.%	0.8	0.95	0.78	0.05	0.3	4.67	0.96
	Leaching efficiency/%	96.55	96.42	88.47	96.46	73.89	0	79.22
Production-2#	Content in material/wt.%	9.92	7.79	2.93	0.67	0.56	2.73	3.39
	Content in 3rd leaching residue/wt.%	0.46	0.53	0.67	0.04	0.28	6.07	1.40
	Leaching efficiency/%	97.91	96.94	89.70	97.45	77.48	0	81.40

4 Conclusions

(1) Compared with the normal material, Ga from the special refinery residue was embedded in the jarosite phase, requiring H_2SO_4 with higher concentration to dissolve Ga.

(2) The dissolution of As, Fe and Ga indicated a similar variation tendency during the oxidation pressure leaching of zinc refinery residues.

(3) A sufficient H_2SO_4 concentration and liquid-to-solid ratio enhanced Ga leaching, whereas higher oxygen partial pressure and reaction temperature promoted the co-precipitation of As, Fe and Ga.

(4) Through weakening the 1st pressure leaching and intensifying the 3rd atmospheric leaching, Ga content in the 3rd residue was lower than 0.05 wt.%, obtaining above 96% of Ga leaching efficiency.

CRediT authorship contribution statement

Wei ZHANG: Investigation, Data curation, Writing − Review & editing; **Shuai RAO:** Methodology, Data curation, Validation, Writing − Original draft; **Li-qing LI:** Methodology, Writing − Review & editing, Supervision; **Xiao-dan GONG:** Methodology, Resources, Data curation; **Cai-gui WU:** Resources, Data curation; **Dong-feng HU:** Resources, Data curation; **Hong-yang CAO:** Formal analysis, Funding acquisition; **Zhi-qiang LIU:** Writing − Review & editing, Supervision, Funding acquisition.

Declaration of competing interest

The authors declare that they have no known competing financial interests or personal relationships that could have appeared to influence the work reported in this paper.

Acknowledgments

This research was financially supported by the National Key Research and Development Project of China (Nos. 2021YFC2902802, 2021YFC2902805, 2021YFC2902602, 2021YFC2902604), the Natural Science Foundation of Guangdong Province, China (No. 2023A1515030145), and Guangdong Academy of Science Special Funds, China (Nos. 2020GDASYL-0104027, 2022GDASZH-2022010104, 2021GDASYL-20210302004).

References

[1] OLIVEIRA R P, BENVENUTI J, ESPINOSA D. A review of the current progress in recycling technologies for gallium and rare earth elements from light-emitting diodes [J]. Renewable and Sustainable Energy Reviews, 2021, 145: 111090.

[2] LU Fang-hai, XIAO Tang-fu, LIN Jian, NING Zeng-ping, LONG Qiong, XIAO Li-hua, HUANG Fang, WANG Wan-kun, XIAO Qing-xiang, LAN Xiao-long, CHEN Hai-yan. Resources and extraction of gallium: A review [J]. Hydrometallurgy, 2017, 174: 105−115.

[3] WEN Kang, JIANG Feng, ZHOU Xiang-yang, SUN Zhao-ming. Leaching of gallium from corundum flue dust using mixed acid solution [J]. Transactions of Nonferrous Metals Society of China, 2018, 28(9):1862−1868.

[4] ZHAO Zhuo, YANG Yong-xiang, XIAO Yan-ping, FAN You-qi. Recovery of gallium from Bayer liquor: A review [J]. Hydrometallurgy, 2012, 125/126: 115−124.

[5] SONG Jia-qi, PENG Cong, LIANG Yan-jie, ZHANG Deng-kai, LIN Zhang, LIAO Yi, WANG Guang-jun. Efficient extracting germanium and gallium from zinc residue by sulfuric and tartaric complex acid [J]. Hydrometallurgy, 2021, 202: 105599.

[6] MACÍAS-MACÍAS K Y, CENICEROS-GÓMEZ A E, GUTIÉRREZ-RUIZ M E, GONZÁLEZ-CHÁVEZ J L, MARTÍNEZ-JARDINES L G. Extraction and recovery of the strategic element gallium from an iron mine tailing [J]. Journal of Environmental Chemical Engineering, 2019, 7(2): 102964.

[7] QIN Shen-jun, SUN Yu-zhuang, LI Yan-heng, WANG Jin-xi, ZHAO Cun-liang, GAO kang. Coal deposits as promising alternative sources for gallium [J]. Earth-Science Reviews, 2015, 150: 95−101.

[8] TAGIYEVA L T, GEIDAROV A A. Separation of aluminum from gallium and vanadium in a sulfate medium by partial neutralization [J]. Russian Journal of Inorganic Chemistry, 2022, 67(2): 183−187.

[9] XUE Bing, WEI Bo-tan, RUAN Liu-xia, LI Fang-fei, JIANG Yin-shan, TIAN Wei-jun, SU Bo, ZHOU Li-ming. The influencing factor study on the extraction of gallium from red mud [J]. Hydrometallurgy, 2019, 186: 91−97.

[10] WU Xue-lan, WU Shun-ke, QIN Wen-qing, MA Xi-hong, NIU Yin-jian, LAI Shao-shi, YANG Cong-ren, JIAO Fen, REN Liu-yi. Reductive leaching of gallium from zinc residue [J]. Hydrometallurgy, 2012, 113/114: 195−199.

[11] ZHANG Kui-fang, QIU Li-li, TAO Jin-zhang, ZHONG Xiao-cong, LIN Zhen-cong, WANG Rui-xiang, LIU Zhi-qiang. Recovery of gallium from leach solutions of zinc refinery residues by stepwise solvent extraction with N235 and Cyanex 272 [J]. Hydrometallurgy, 2021, 205: 105722.

[12] ZHAO Ze-sen, CUI Li, GUO Yan-xia, GAO Jian-ming, LI Hui-quan, CHENG Fang-qin. A stepwise separation process for selective recovery of gallium from hydrochloric acid leach liquor of coal fly ash [J]. Separation and Purification Technology, 2021, 265: 118455.

[13] ZHAO Ze-sen, CUI Li, GUO Yan-xia, LI Hui-quan, CHENG Fang-qin. Recovery of gallium from sulfuric acid leach liquor of coal fly ash by stepwise separation using P507 and Cyanex 272 [J]. Chemical Engineering Journal, 2020, 381: 122699.
[14] ZHOU Ling-zhi, CHEN Shao-chun. Scattered metals extraction metallurgy [M]. Beijing: Metallurgical Industry Press, 2008. (in Chinese)
[15] ABKHOSHK E, JORJANI E, AL-HARAHSHEH M S, RASHCHI F, NAAZERI M. Review of the hydrometallurgical processing of non-sulfide zinc ores [J]. Hydrometallurgy, 2014, 149: 153−167.
[16] DUTRIZAC J E, CHEN T T. The behaviour of gallium during jarosite precipitation [J]. Canadian Metallurgical Quarterly, 2000, 39(1): 1−14.
[17] KASHYAP V, TAYLOR P, KARUMB E T, CHESHIRE M. Application of zinc ferrite reduction in the extraction of Zn, Ga and In from zinc refinery residue [J]. Minerals Engineering, 2021, 171: 107078.
[18] KASHYAP V, TAYLOR P. Extraction and recovery of zinc and indium from residue rich in zinc ferrite [J]. Minerals Engineering, 2022, 176: 107364.
[19] LIU Fu-peng, LIU Zhi-hong, LI Yu-hu, WILSON B P, LUNDSTRÖM M. Recovery and separation of gallium(III) and germanium(IV) from zinc refinery residues. Part I: Leaching and iron(III) removal [J]. Hydrometallurgy, 2017, 169: 564−570.
[20] LIU Fu-peng, LIU Zhi-hong, LI Yu-hu, LIU Zhi-yong, LI Qi-hou. Leaching mechanism of zinc powder replacement residue containing gallium and germanium by high pressure acid leaching [J]. The Chinese Journal of Nonferrous Metals, 2014, 24(4): 1091−1098. (in Chinese)
[21] RAO Shuai, WANG Dong-xing, LIU Zhi-qiang, ZHANG Kui-fang, CAO Hong-yang, TAO Jin-zhang. Selective extraction of zinc, gallium, and germanium from zinc refinery residue using two stage acid and alkaline leaching [J]. Hydrometallurgy, 2019, 183: 38−44.
[22] RAO Shuai, LIU Zhi-qiang, WANG Dong-xing, CAO Hong-yang, ZHU Wei, ZHANG Kui-fang, TAO Jin-zhang. Hydrometallurgical process for recovery of Zn, Pb, Ga and Ge from Zn refinery residues [J]. Transactions of Nonferrous Metals Society of China, 2021, 31(2): 555−564.
[23] LIU Fu-peng, LIU Zhi-hong, LI Yu-hu, WILSON B P, LUNDSTRÖM M. Extraction of Ga and Ge from zinc refinery residues in $H_2C_2O_4$ solutions containing H_2O_2 [J]. International Journal of Mineral Processing, 2017, 163: 14−23.
[24] WANG Yu-fang, WANG Hai-bei, LI Xiang-liang, ZHENG Chao-zhen. Study on the improvement of the zinc pressure leaching process [J]. Hydrometallurgy, 2020, 195: 105400.
[25] LIU Fu-peng, LIU Zhi-hong, LI Yu-hu, LIU Zhi-yong, LI Qi-hou, ZENG Li. Extraction of gallium and germanium from zinc refinery residues by pressure acid leaching [J]. Hydrometallurgy, 2016, 164: 313−320.
[26] ZHANG Wei, LI Li-qing, LIU Ye-ping, ZHANG Jun-feng, WU Cai-gui, GONG Xiao-dan. Leaching of valuable metals from gallium−germanium residue by two-stage counter-current pressure leaching process [J]. Hydrometallurgy of China, 2021, 40(4): 289−293. (in Chinese)
[27] ZHANG Wei, GONG Xiao-dan, ZHOU Ke-hua, WU Cai-gui, ZHANG Deng-kai, CHEN Long-yi, DENG Meng-li. Production practice of zinc powder replacement Ga and Ge slag by pressure oxidation leaching [J]. Nonferrous Metals Science and Engineering, 2020, 11(5): 142−147. (in Chinese)
[28] LIANG Duo-qiang, WANG Ji-kun, WANG Yun-hua. Difference in dissolution between germanium and zinc during the oxidative pressure leaching of sphalerite [J]. Hydrometallurgy, 2009, 95(1): 5−7.
[29] JIANG Dao-yan, LIU Zhi-yong, LIU Zhi-hong. Oxidation of As(III) by pressurized oxygen and the simultaneous precipitation of As(V) as scorodite in acidic sulfate solutions [J]. Chemical Engineering Journal, 2022, 447: 137395.

锌粉置换渣浸出过程中镓的溶解行为及改善方法

张 伟[1,2]，饶 帅[3]，李立清[1]，宫晓丹[2]，吴才贵[2]，胡东风[2]，曹洪杨[3]，刘志强[3]

1. 江西理工大学 材料冶金化学学部，赣州 341000；
2. 深圳市中金岭南有色金属股份有限公司 丹霞冶炼厂，韶关 512325；
3. 广东省科学院 资源利用与稀土开发研究所，广州 510650

摘 要：针对丹霞冶炼厂锌粉置换渣浸出过程中镓浸出率偏低问题，采用 ICP−AES、XRD 与 SEM−EDS 对不同批次锌粉置换渣化学成分、物相与形貌进行详细分析。与正常生产锌粉置换渣相比，异常锌粉置换渣中镓主要赋存于黄钾铁矾之中，造成镓浸出困难。对锌粉置换渣氧压浸出过程进行分析，镓、砷和铁溶出规律较为一致：增大硫酸浓度和液固比有利于镓、铁和砷的浸出，但提高温度和氧气分压对镓、铁和砷溶出不利。依据上述研究结果，提出强化镓浸出效率的改善措施，弱化一段氧压浸出(分别降低反应温度和压缩空气总压至 90 ℃和 0.2 MPa)与强化三段常压浸出(分别提高硫酸浓度和反应温度至 160 g/L 和 85 ℃)，镓的浸出效率由 77.83%提高至 96.46%。

关键词：溶解行为；锌粉置换渣；镓；黄钾铁矾；臭葱石

(Edited by Wei-ping CHEN)